HHS Public Access

Author manuscript

Cancer Res. Author manuscript; available in PMC 2017 May 01.

Published in final edited form as:

Cancer Res. 2016 May 1; 76(9): 2791–2801. doi:10.1158/0008-5472.CAN-15-1975.

Heparanase 2 attenuates head and neck tumor vascularity and growth

Miriam Gross-Cohen[1], **Sari Feld**[1], **Ilana Doweck**[2], **Gera Neufeld**[1], **Peleg Hasson**[3], **Gil Arvatz**[1], **Uri Barash**[1], **Inna Naroditsky**[4], **Neta Ilan**[1], and **Israel Vlodavsky**[*,1]

[1]Cancer and Vascular Biology Research Center, the Bruce Rappaport Faculty of Medicine, Technion, Haifa 31096, Israel

[2]Department of Otolaryngology, Head and Neck Surgery, Carmel Medical Center, Haifa, Israel

[3]Department of Anatomy and Cell Biology, the Bruce Rappaport Faculty of Medicine, Technion, Haifa 31096, Israel

[4]Department of Pathology, Rambam Health Care Campus, Haifa, Israel

Abstract

The endoglycosidase heparanase specifically cleaves the heparan sulfate (HS) side chains on proteoglycans, an activity that has been implicated strongly in tumor metastasis and angiogenesis. Heparanase-2 (Hpa2) is a close homolog of heparanase that lacks intrinsic HS-degrading activity but retains the capacity to bind HS with high affinity. In head and neck cancer patients, Hpa2 expression was markedly elevated, correlating with prolonged time to disease recurrence and inversely correlating with tumor cell dissemination to regional lymph nodes, suggesting that Hpa2 functions as a tumor suppressor. The molecular mechanism associated with favorable prognosis following Hpa2 induction is unclear. Here we provide evidence that Hpa2 overexpression in head and neck cancer cells markedly reduces tumor growth. Restrained tumor growth was associated with a prominent decrease in tumor vascularity (blood and lymph vessels), likely due to reduced Id1 expression, a transcription factor highly implicated in VEGF-A and VEGF-C gene regulation. We also noted that tumors produced by Hpa2 overexpressing cells are abundantly decorated with stromal cells and collagen deposition, correlating with a marked increase in lysyl oxidase expression. Notably, heparanase enzymatic activity was unimpaired in cells overexpressing Hpa2, suggesting that reduced tumor growth is not caused by heparanase regulation. Moreover, growth of tumor xenografts by Hpa2-overexpressing cells was unaffected by administration of a monoclonal

[*]To whom correspondence should be addressed: Israel Vlodavsky, Cancer and Vascular Biology Research Center, Bruce Rappaport Faculty of Medicine, Technion, P. O. Box 9649, Haifa 31096, Israel, Phone: 972-4-8295410; Fax: 972-4-8510445, ; Email: Vlodavsk@mail.huji.ac.il.

Conflict of interest: The authors have no potential conflict of interest to declare

Authors' contribution:
Conception and design: IV, NI
Development of methodology: MG, NI
Acquisition of data: MG, SF, UB, NI
Analysis and interpretation of data: MG, NI, GN, PH, IV, IN, ID
Writing, review, and/or revision of the manuscript: MG, NI, IV, GN, PH
Administrative, technical, or material support: GN, PH
Study supervision: IV

antibody that targets the heparin binding domain of Hpa2, implying that Hpa2 function does not rely on heparanase or heparin sulfate

Keywords

Heparanase; Hpa2; vascularity; LOX; tumorigenicity

Introduction

Heparanase is an endoglycosidase that specifically cleaves heparan sulfate (HS) side chains, a class of glycosaminoglycans abundantly present in the extracellular matrix (ECM) and on the cell surface. Heparanase activity is strongly implicated in tumor angiogenesis and metastasis attributed to remodeling of the subepithelial and subendothelial basement membranes (1, 2). Augmented level of heparanase was documented in an increasing number of human carcinomas and hematological malignancies (3, 4). In many cases, heparanase induction correlates with increased tumor metastasis, vascular density, and shorter survival post-operation, thus providing a strong clinical support for the pro- tumorigenic function of the enzyme (4–6). These studies depict compelling evidence for the clinical relevance of heparanase, making it an attractive target for the development of anti-cancer drugs (5, 7, 8). Cloning of a single human heparanase cDNA sequence was independently reported by several groups (9–12) implying that one active heparanase enzyme exists in mammals. Further analysis of human genomic DNA led researchers to conclude that the heparanase gene is unique, and that the existence of related proteins is unlikely. Based on amino acid sequence, McKenzie and colleagues nonetheless reported the cloning of heparanase homolog termed heparanase 2 (Hpa2) (13). Unlike heparanase, Hpa2 lacks intrinsic HS-degrading activity, the hallmark of heparanase, but retains the capacity to bind heparin/HS (14). In fact, Hpa2 exhibits even higher affinity towards heparin/HS than heparanase, suggesting that Hpa2 may inhibit heparanase activity by competition for the HS substrate (14). Clinically, Hpa2 expression was markedly elevated in head and neck carcinoma patients, correlating with prolonged time to disease recurrence (follow-up to failure) and inversely correlating with tumor cell dissemination to regional lymph nodes, suggesting that Hpa2 functions as a tumor suppressor (14). The molecular mechanism associated with favorable prognosis following Hpa2 over expression is unclear. Here, we provide evidence that Hpa2 over expression in head and neck cancer cells markedly reduces tumor growth. Restrained tumor growth was associated with a prominent reduction in tumor vascularity (blood and lymph vessels) likely due to reduced Id1 expression, a transcription factor highly implicated in VEGF-A and VEGF-C gene regulation (15). Notably, heparanase enzymatic activity was not impaired in cells over expressing Hpa2, suggesting that reduced tumor growth is not due to heparanase regulation. Moreover, growth of tumor xenografts produced by Hpa2 over-expressing cells was not affected by a monoclonal antibody that targets a heparin binding domain of Hpa2, implying that Hpa2 functions in heparanase-, and HS-independent manner.

Materials and methods

Cells and cell culture, immunoblotting, and heparanase activity assay

Cal27 tongue carcinoma and FaDu pharyngeal carcinoma cells have been described previously (16–18). Cells were grown in Dulbecco's modified Eagle's medium (Biological Industries, Beit Haemek, Israel) supplemented with 10% fetal bovine serum and antibiotics. Cells were passed in culture no more than 2 months after being thawed from authentic stocks. Cells were infected with control empty vector (Vo) or Hpa2 gene construct, selected with Puromycin (2 μg/ml; Invitrogen), expended and pooled. Cell clones were isolated by limiting dilution and clones exhibiting higher Hpa2 expression vs. the pool of cells were evaluated by immunoblotting, carried out essentially as described (14). Preparation of dishes coated with sulfate labeled ECM and determination of heparanase enzymatic activity (i.e., release of sulfate labeled HS degradation fragments) were carried out essentially as described previously (14).

Antibodies and reagents

Anti-Hpa2 polyclonal (Ab 58) and monoclonal (20c5, 1c7) antibodies have been described previously (14). Immunohistochemical-grade anti-LOX and anti-LOXL2 polyclonal antibodies have been described elsewhere (19, 20). Antibodies directed against Ki67, LYVE-1, LOX, cytokeratin 13, cytokeratin 15, β3-tubulin, cleaved-caspase 3, HIF-1 alpha, and carbonic anhydrase IX were purchased from Abcam (Cambridge, UK); Rat anti-mouse CD31 was from Dianova (Hamburg, Germany); Anti VEGF-A and anti VEGF-C antibodies were from Santa Cruz Biotechnology (Santa Cruz, CA). Anti-actin and anti-smooth muscle actin (SMA) monoclonal antibodies, Masson's/Trichrome staining kit and beta-3-aminopropionitrile fumarate (BAPN) were purchased from Sigma. Human Id1 gene construct was purchased from Addgene (Cambridge, MA).

Real time-PCR

Real time-PCR analyses were performed using ABI PRISM 7000 Sequence Detection System employing SYBR Green PCR Master Mix (Applied Biosystems, Foster City, CA). The following primers were used:

Actin F: 5′-CGCCCCAGGCACCAGGGC, R: 5′-GCTGGGGTGTTGAAGGT;

VEGF-A F: 5′-TCTACCTCCACCATGCCAAGT, R: 5′ TGTCCACCAGGGTCTCGATT;

VEGF-C F: 5′-GCCAACCTCAACTCAAGGAC, R: 5′-CCCACATCTGTAGACGGACA;

LOX F: 5′-GTACGTGCAGAAGATGTCC, R: 5′-CTGAGCAGCACCCTGTGATC;

LOXL2 F: 5′-TCGAGGTTGCAGAATCCGATT, R 5′ TTCCGTCTCTTCGCTGAAGGA;

Id1 F: 5′-CTGCTCTACGACATGAACGG, R 5′-GAAGGTCCCTGATGTAGTCGAT.

Tumorigenicity and immunohistochemistry

Cells were detached with trypsin/EDTA, washed with PBS, and brought to a concentration of 5×10^7 cells/ml. Cell suspension (5×10^6/0.1ml) was inoculated subcutaneously at the right flank of 6 week-old NOD/SCID mice. Xenografts size was determined by externally measuring tumors in 2 dimensions using a caliper. At the end of the experiment, mice were sacrificed; tumor xenografts were removed, weighed, and fixed in formalin. Paraffin-embedded 5 μm sections were subjected to immunostaining with the indicated antibody using the Envision kit according to the manufacturer's (Dako) instructions, as described previously (14). Immunocytochemistry was carried out essentially as described (21). Lymph and blood vessels density was quantified by the Image Pro software or were counted under light microscope at high (×40) magnification.

Statistics

Data are presented as means ± SE. Statistical significance was analyzed by 2-tailed Student's *t* test. Values of $P < 0.05$ were considered significant. Data sets passed D'Agostino-Pearson normality (GraphPad Prism 5 utility software). All experiments were repeated at least 3 times with similar results.

Results

Hpa2 over expression attenuates tumor growth

In order to reveal the function of Hpa2 in head and neck cancer, FaDu pharyngeal carcinoma cells were infected with control (Vo) or Hpa2 gene constructs and expression was confirmed by immunoblotting (Suppl. Fig. S1A; Pool) and immunofluorescent staining (Suppl. Fig. S1B). Tumor xenografts produced by FaDu cells over expressing Hpa2 were markedly smaller by volume and weight compared with control tumors (Fig. 1A; p=0.001). Histological examination showed that xenografts produced by control cells were highly necrotic (Fig. 1B, left panels). In contrast, xenografts produced by cells over expressing Hpa2 were by far less necrotic and were decorated with large cysts (Fig. 1B, right panels). Similar robust cysts formation was evident in Cal27 cells over expressing Hpa2 (Fig. 1B, lower panels). In head and neck cancer patients, high levels of Hpa2 expression were associated with reduced lymph nodes metastasis and prolonged survival rates (14). We therefore examined the occurrence of lymph vessels in tumor xenografts produced by control and Hpa2 over expressing cells. We observed a significant 2–3 fold decrease in lymphangiogenesis following Hpa2 over expression (Fig. 1C, D; p=0.002), associated with a comparable decrease in the expression of VEGF-C (Fig. 1D, lower panel), a predominant factor for the proliferation of lymphatic endothelial cells (22, 23).

Tumor growth and vascularity are markedly reduced by Hpa2 over expressing cell clones

In order to further delineate the impact of Hpa2 on tumor growth, we selected cell clones that exhibit high levels of Hpa2 expression. Three such cell clones were isolated from Hpa2 infected cells (clones #6, 60, 64; Suppl. Fig. S1A) and their tumorigenic capacity was compared to that of three randomly selected control cell clones (clones #3, 5, 8). Tumor xenografts produced by Hpa2 over expressing clones were strikingly, 10-fold smaller

compared with xenografts produced by control cell clones, decrease that is statistically highly significant (Fig. 2A; Suppl. Fig. S1C). Proliferating, Ki67-positive cells were detected in the entire non-necrotic tumor mass produced by control clones (Fig. 2B, left panels). Endothelial cells and tumor cells residing in lymphatics were also stained positive for Ki67 in control tumors (Suppl. Fig. S2A). In contrast, Ki67 reactivity was restricted to the tumor periphery in tumors produced by Hpa2 clones (Fig. 2B, right panels) and was decreased significantly even in these areas (Fig. 2B, lower panel). In addition, tumors produced by Hpa2 clones exhibited higher levels of apoptotic cell death evident by caspase-3 staining (Suppl. Fig. S2B), altogether attenuating tumor growth. Histologically, tumors produced by control cell clones exhibited massive areas of necrosis vs. large cysts that decorated the tumors produced by Hpa2 clones (Fig. 2C), in agreement with the histological phenotype of tumors produced by cell pools (Fig. 1B). Careful pathological examination revealed that tumors produced by Hpa2 clones exhibit higher degree of differentiation (Fig. 2C, right panels), and this was confirmed by a marked increase in cytokeratin 13 and cytokeratin 15 immunostaining (Fig. 2D) and immunoblotting (Suppl. Fig. S2C). Furthermore, a noticeable decrease in lymph vessels (positive for LYVE-1) density was quantified in tumor xenografts produced by Hpa2 clones compared with controls (Fig. 3A, second and fifth left panels), associating with a 3-fold decrease in VEGF-C expression levels (Fig. 3B). This agrees with decreased lymphangiogenesis and VEGF-C expression observed in the cell pools (Fig. 1C, D). Notably, while tumor cells were readily detected within lymph vessels of control tumors (Fig. 3A, second left panels), Hpa2 over expression resulted not only in fewer lymph vessels but also reduced tumor load in lymphatics (Fig. 3A, second right panels). While this observation is in accordance with our previous experimental (Fig. 1C,D) and clinical results (14), it cannot explain the robust attenuation of tumor growth. We therefore examined also the density of blood vessels in tumors produced by control and Hpa2 over expressing cells. We found that blood vessel density was prominently reduced in tumors produced by Hpa2 over expressing cells compared with control tumors (Fig. 3A, third and fifth-right panels), associating with a comparable decrease in VEGF-A expression (Fig. 3C; Suppl. Fig. S1D). Consequently, tumors produced by Hpa2 clones exhibited augmented tumor hypoxia evident by increased HIF-1α (Fig. 3A, fourth panels) and carbonic anhydrase IX (CAIX; Suppl. Fig. S2D) staining intensity.

Hpa2 enhances collagen deposition and LOX induction

Histological examination revealed that tumors produced by Hpa2 cells are decorated extensively with host, stromal cells (Suppl. Fig. S3A). Masson's/Trichrome staining showed a marked increase in collagen staining following Hpa2 over expression (Fig. 4, upper panels, blue). A similar increase in collagen staining was observed in tumors produced by Cal27 cells over expressing Hpa2 (Suppl. Fig. S3B). We therefore examined the expression of lysyl oxidase (LOX), an enzyme that is strongly implicated in collagen deposition and tissue fibrosis (24, 25). We found a prominent increase in LOX immunostaining in cancer cells that surround the stromal elements within tumors produced by Hpa2 clones compared with control (Fig. 4A, second panels; Suppl. Fig. S4A, upper panels). LOX up-regulation by Hpa2 was further ascertained by real-time PCR (Fig. 4B). In contrast, the expression of lysyl oxidase-like 2 (LOXL2) was decreased in Hpa2 clones (Fig. 4C). Notably, however, LOXL2

was predominantly localized to the nuclei of cancer (Fig. 4A, lower right panels) and stromal cells (Suppl. Fig. S3C, arrows). Similar phenotypes were observed in tumors produced by Cal27 cells over expressing Hpa2 (Suppl. Fig. S3B, lower panels).

Hpa2 mode of action

In order to reveal the mechanism underlying the potent suppression of tumor growth by Hpa2 we first evaluated heparanase activity in control and Hpa2 over expressing cells, because heparanase exhibits pro-tumorigenic properties in many types of cancers including head and neck (26), and Hpa2 can inhibit heparanase enzymatic activity (14). Notably, heparanase activity appeared unchanged in control vs. Hpa2 over expressing cells (Fig. 5A), suggesting that the decrease in tumor growth by Hpa2 is not due to heparanase inhibition. Despite its lack of HS-degrading activity, Hpa2 exhibits high affinity towards heparin/HS (14). We therefore sought to examine whether binding and clustering of HS proteoglycans (HSPG) by Hpa2 on the cell surface is responsible for tumor suppression. To this end, we screened a panel of anti-Hpa2 monoclonal antibodies (mAb) for inhibition of cellular binding of Hpa2 shown previously to be mediated by cell membrane HSPG such as syndecans (14). We found that mAb 1c7 efficiently inhibits cellular binding of Hpa2 in a dose-dependent manner (Fig. 5B), suggesting that this mAb targets a functional HS-binding domain of Hpa2. Importantly, tumor growth was not altered by administration of mAb 1c7 to mice inoculated with Hpa2 clones (Fig. 5C; Suppl. Fig. S5A). Interestingly, the formation of cysts within tumors appeared to be increased in mice treated with mAb 1c7 (Fig. 5C; Suppl. Fig. S5A). Immunoblotting revealed reduced levels of VEGF-A in Hpa2 over expressing clones (Fig. 5D upper panel, - ; Suppl. Fig. S1D), in agreement with real-time PCR (Fig. 3C), but VEGF-A levels were not affected by treatment with mAb 1c7 (Fig. 5D, upper panel, +). Taken together, it appears that inhibition of tumor growth and vascularity by Hpa2 does not involve regulation of heparanase activity or the activation of cell membrane HSPG. Furthermore, treatment with BAPN, which inhibits the enzymatic activity of all lysyl-oxidases (27) reduced tumor fibrosis (i.e., collagen content) but had no effect on tumor size (Fig. 5E; Suppl. Fig. S5B), implying that reduced tumor growth by cells over expressing Hpa2 is not due to the elevation of LOX activity. We therefore considered the reduced tumor vascularity as the main cause for tumor growth inhibition by Hpa2. Interestingly, we found that expression of Id1, a transcription factor implicated in the induction of VEGF-A and VEGF-C gene transcription (15, 28), is reduced in Hpa2 over expressing cells (Fig. 6A). Over expression of Id1 in Hpa2 clones (Fig. 6B) resulted in a 2.5–3-fold increase in tumor growth (Fig. 6C) and a comparable increase in tumor vascularity (Fig. 6D; Suppl. Fig. S5C), implying that down regulation of Id1 mediates, at least in part, the tumor suppressor function of Hpa2.

Discussion

Compelling pre-clinical and clinical evidences tie heparanase with cancer initiation and progression (8, 29–31), making it a promising drug target (5, 7). In striking contrast, the biological significance of its close homolog Hpa2 in tumorigenesis is largely obscure. We have reported previously that Hpa2 levels are increased in head and neck carcinoma compared with adjacent normal tissue, and that patients with high levels of Hpa2 are

endowed with reduced lymph node metastasis and prolonged survival rates (14). Similarly, increased Hpa2 expression was associated with prolonged survival of gastric cancer patients (32) but the mechanism underlying this favorable effect has not been resolved yet. Here, we provide evidence that high levels of Hpa2 are associated with reduced lymph vessel density. This was noted in pool of FaDu cells infected with Hpa2 gene construct (Fig. 1C, D) and was most evident in three different cell clones selected for higher levels of Hpa2 expression (Fig. 3A). Importantly, these clones express Hpa2 levels comparable with patients exhibiting high levels of Hpa2, [(14); Suppl. Fig. S4B] and are thus considered relevant to the disease. Lymph-angiogenesis is significant clinically for many types of cancers but most appealing in head and neck cancer because lymph node metastasis is the most important clinical parameter for this malignancy (33). We found reduced lymph vessel density in Hpa2 tumors combining with a comparable decrease in VEGF-C expression (Fig. 3B), a most potent pro-lymphatic mediator secreted by tumor cells (34). While decreased VEGF-C expression and lymph-angiogenesis by Hpa2 nicely agrees with the clinical results (14, 32), it cannot explain the prominent decrease in tumor growth following Hpa2 over expression (Fig. 2A; Suppl. Fig. S1C). Notably, we found that not only VEGF-C but also VEGF-A expression is reduced by Hpa2 (Figs. 3C & 5D; Suppl. Fig. S1D), associating with reduced blood vessel density (Fig. 3A) that likely attenuates tumor growth. This agrees with increased levels of hypoxia in tumors produced by Hpa2 clones, evident by higher levels of HIF-1α and carbonic anhydrase IX (Fig. 3A; Supp. Fig. S2D), well recognized markers of hypoxic conditions. Tumors produced by Hpa2 over-expressing clones appeared significantly less necrotic despite being poorly vascularized. This is due to a marked decrease in tumor cell proliferation (Fig. 2B) and increased apoptosis (Suppl. Fig. S2B), thus balancing tumor mass and blood vessel density closer to the ratio occurring in normal tissues.

The mechanism responsible for VEGF-A and VEGF-C down regulation is not entirely clear but likely involves Id1. This transcription factor is implicated in the induction of VEGF-A and VEGF-C gene expression (35, 36) and is decreased following Hpa2 over expression (Fig. 6A). Notably, transfection of Hpa2 clones with Id1 gene construct, resulting in two-folds increase in its mRNA levels (not shown), restored tumor vascularity and growth (Fig. 6C, D; Suppl. Fig. S5C), thus supporting the notion that reduced Id1 levels underlie tumor inhibition by Hpa2 and suggesting that modest changes in the expression levels of this transcription factor are highly effective in modulating tumor progression. This appears relevant clinically, because Id1 expression has been shown to be elevated in a variety of primary human tumors including head and neck cancer, correlating with increased tumor aggressiveness (37). It should be noted that Id1 is thought to function as a cellular proto-oncogene (37) and regulates the transcription of several other genes implicated in tumor growth such as metalloproteinases and integrins (35). Decreased Id1 gene expression by Hpa2 may therefore affect tumor growth also by means other than reduced vascularity. Interestingly, we found that the expression of cytokeratin 13 & 15 was reduced markedly in tumors produced by Hpa2 clones over expressing Id1 (Suppl. Fig. S6), while LOX expression was unchanged (Suppl. Fig. S7, lower panels). Accordingly, collagen deposition, evident by Masson's/Trichrome staining, was not affected by Id1 over expression (Suppl. Fig. S7, third panels), but appeared disrupted in the large necrotic areas that accompanied accelerated tumor growth (Suppl. Fig. S7, upper and second panels), suggesting that

collagen deposition preceded tumor necrosis. These results may imply that cytokeratins are also regulated, directly or indirectly, by Id1. An inverse correlation between Id1 levels and cytokeratin expression was also reported in ovarian carcinoma cells (38).

Over expression of Hpa2 affect the resulting tumors in several aspects other than reduced tumor vascularity. Despite the reduced vascularity, tumor xenografts produced by Hpa2 over expressing cells were by far less necrotic but rather contained large cysts structures. These structures, observed in FaDu and Cal27 cell models (Fig. 1B, Fig. 2C), were negative for endothelial cell marker (CD31, Suppl. Fig. S4A, right lower panel), thus nullifying their being abnormal vessels. Cysts are most often non-malignant structures but can appear in primary tumors and metastases (39). The molecular mechanism responsible for cyst formation by Hpa2 is obscure but may be related to increased cellular differentiation. Histological examination revealed that tumor xenografts produced by Hpa2 over expressing cells and clones exhibit higher degree of differentiation (Fig. 2C) and this was evidently confirmed by a marked increase in cytokeratins levels (Fig. 2D, Suppl. Fig. S2C). Cytokeratin 15 staining was most intense in cells lining, or in close proximity with the cyst structure (Fig. 2D, lower panels), but the cause and relationship between increased cell differentiation and cyst formation is yet to be resolved. Alternatively, increased formation of cyst structures in Hpa2 tumors may possibly reflect adaptation to reduced lymph vessels density and the formation of edema.

We have also noted that tumors produced by Hpa2 clones had far more nerve bundles than control tumors (β3-tubulin; Suppl. Fig. S4A, second panels). While the contribution of neurogenesis to tumorigenesis is questionable (40), a possible role for Hpa2 in neurogenesis appears relevant to urofacial syndrome (UFS). This congenital disorder features somatic motor neuropathy, obvious in the face but occasionally more widespread, and an autonomic neuropathy causing bladder dysfunction leading to renal failure (41). Notably, biallelic mutation in the *HPSE2* gene is held responsible for some cases of UFS in families from different ethnic groups (42–44), resulting in frameshift or nonsense, postulated functionally null, Hpa2 variants (45). Moreover, mice carrying mutant Hpa2 exhibit bladder dysfunction (44, 46), associating with increased bladder fibrosis (46). The relevance of our findings with Hpa2 over expressing head and neck carcinoma cells (i.e., increased cell differentiation, neurogenesis, LOX expression) to UFS and the lethality phenotype of Hpa2 mutant mice (46) are yet to be resolved.

Augmented collagen deposition was observed in tumor xenografts produced by Hpa2 clones (Fig. 4), correlating with a marked increase in LOX expression (Fig. 4). This enzyme catalyzes the cross-linking of collagen and/or elastin in the ECM, and is highly implicated in ECM remodeling and tissue fibrosis (24, 25). In tumorigenesis, LOX was first proposed to act as a tumor suppressor, inhibiting the transformation effect of HRAS. Subsequent studies revealed nonetheless that LOX plays a far more complex role in cancer. For example, the LOX propeptide (LOX-PP) domain has been shown to bear tumor-suppressor activity, while the active enzyme is thought to promote metastasis (27, 47). Tumor suppressor properties have also been attributed to the LOX-like 2 enzyme, LOXL2. For example, a significant decrease in LOXL2 expression was observed in prostate and non-small-lung cancers compared with matched normal tissue (27) and low LOXL2 levels were associated with a

more advanced pathological TNM stage and poorly differentiated lung adenocarcinomas (48). Not only the expression levels but also the cellular localization of LOXL2 appears important clinically. LOXL2 was noted to reside in the nucleus of normal esophagus, and esophageal cancer patients having nuclear LOXL2 survive longer than patients with cytoplasmic LOXL2 (49). We found that LOXL2 localizes to the nucleus of Hpa2 over expressing cancer cells (Fig. 4) and cells that comprise the tumor microenvironment (Suppl. Fig. S3C). This agrees with the notion that nuclear localization of LOXL2 attenuates tumor growth by transcriptional regulation of tumor (50) and stromal cells that may affect tumor growth (51). Interestingly, administration of the LOX inhibitor BAPN to the drinking water of mice inoculated with Hpa2 clones did not reverse the strong attenuation of tumor growth by Hpa2 (Fig. 5E; Suppl. Fig. S5B). This may imply that LOX functions extracellularly in a manner that does not involve enzymatic activity (52), or that nuclear LOXL2 is responsible for tumor attenuation. It should be noted that in contrast with the above examples, other studies find that LOX and LOXL2 promote tumor growth and metastasis, making these enzymes a target for the development of anti-cancer therapeutics (24, 27). Clearly, more work is required to delineate the mode by which Hpa2 regulates LOX and LOXL2 expression and cellular localization, the clinical significance of LOX/LOXL2 expression and localization in head and neck cancer, and the implication of a Hpa2-TGFβ-LOX axis (20, 53) on tumor growth, metastasis and fibrosis. It should be noted that while hypoxic conditions have been reported to induce LOX expression (54), increased LOX transcription was noted in Hpa2 cells grown in vitro under normoxic conditions (Fig. 4B), suggesting that Hpa2 regulates LOX gene expression directly.

The mode by which Hpa2 exerts its tumor suppressor properties is not entirely clear. An instrumental tool for deciphering this question was the finding that mAb 1c7 inhibits cellular binding of Hpa2 (Fig. 5B). Like heparanase, Hpa2 is subjected to rapid and efficient cellular binding (14). This process is due primarily to the interaction of heparanase/Hpa2 with HSPG on the cell surface because addition of heparin to cell cultures competes with cell membrane HS, resulting in accumulation of heparanase/Hpa2 in the cell culture medium (14). Unlike heparanase (18), the heparin binding domains of Hpa2 have not been characterized yet. However, the ability of mAb 1c7 but no other anti-Hpa2 mAbs, to efficiently block cellular binding of Hpa2 (Fig. 5B) strongly implies that this mAb targets a functional domain required for the interaction of Hpa2 with HS. The consequence of the high affinity interaction of Hpa2 with cell membrane HS has not been sufficiently resolved but likely affects cellular behavior (i.e., cell adhesion) (55). Notably, tumor growth inhibition by Hpa2 does not appear to involve HS because treatment with mAb Ic7 did not affect tumor size (Fig. 5C; Suppl. Fig. S5A). Moreover, heparanase activity appeared practically identical in control and Hpa2 over expressing cells (Fig. 5A). These results may suggest that Hpa2 exerts its tumor suppressor properties in a HS- and heparanase activity-independent manner, possibly involving as yet unrecognized Hpa2-binding protein.

Taken together, our results support the notion that Hpa2 functions as a tumor suppressor in head and neck cancer. Moreover, we provide mechanistic insights to this function of Hpa2 and describe for the first time that Hpa2 modulates gene transcription and thereby affects tumor vascularity, growth and fibrosis in apparently heparanase-activity-, and HS-independent manners, thus expanding Hpa2 repertoire and mode of action.

Supplementary Material

Refer to Web version on PubMed Central for supplementary material.

Acknowledgments

This study was supported by research grants awarded to I.V. by the Israel Science Foundation (grant 601/14); National Cancer Institute, NIH (grant CA106456); the United States-Israel Binational Science Foundation (BSF); the Israel Cancer Research Fund (ICRF); and the Rappaport Family Institute Fund. I. Vlodavsky is a Research Professor of the ICRF.

References

1. Dempsey LA, Brunn GJ, Platt JL. Heparanase, a potential regulator of cell-matrix interactions. Trends Biochem Sci. 2000; 25:349–51. [PubMed: 10916150]
2. Parish CR, Freeman C, Hulett MD. Heparanase: a key enzyme involved in cell invasion. Biochim Biophys Acta. 2001; 1471:M99–108. [PubMed: 11250066]
3. Vlodavsky I, Beckhove P, Lerner I, Pisano C, Meirovitz A, Ilan N, et al. Significance of heparanase in cancer and inflammation. Cancer Microenviron. 2012; 5:115–32. [PubMed: 21811836]
4. Vreys V, David G. Mammalian heparanase: what is the message? J Cell Mol Med. 2007; 11:427–52. [PubMed: 17635638]
5. Hammond E, Khurana A, Shridhar V, Dredge K. The role of heparanase and sulfatases in the modification of heparan sulfate proteoglycans within the tumor microenvironment and opportunities for novel cancer therapeutics. Front Oncol. 2014; 4:195. [PubMed: 25105093]
6. Ilan N, Elkin M, Vlodavsky I. Regulation, function and clinical significance of heparanase in cancer metastasis and angiogenesis. Intl J Biochem & Cell Biol. 2006; 38:2018–39.
7. Vlodavsky I, Ilan N, Naggi A, Casu B. Heparanase: structure, biological functions, and inhibition by heparin-derived mimetics of heparan sulfate. Curr Pharm Des. 2007; 13:2057–73. [PubMed: 17627539]
8. Weissmann M, Arvatz G, Horowitz N, Feld S, Naroditsky I, Zhang Y, et al. Heparanase-neutralizing antibodies attenuate lymphoma tumor growth and metastasis. Proc Natl Acad Sci USA. 2016; 113:704–709. [PubMed: 26729870]
9. Hulett MD, Freeman C, Hamdorf BJ, Baker RT, Harris MJ, Parish CR. Cloning of mammalian heparanase, an important enzyme in tumor invasion and metastasis. Nat Med. 1999; 5:803–9. [PubMed: 10395326]
10. Kussie PH, Hulmes JD, Ludwig DL, Patel S, Navarro EC, Seddon AP, et al. Cloning and functional expression of a human heparanase gene. Biochem Biophys Res Commun. 1999; 261:183–7. [PubMed: 10405343]
11. Toyoshima M, Nakajima M. Human heparanase. Purification, characterization, cloning, and expression. J Biol Chem. 1999; 274:24153–60. [PubMed: 10446189]
12. Vlodavsky I, Friedmann Y, Elkin M, Aingorn H, Atzmon R, Ishai-Michaeli R, et al. Mammalian heparanase: gene cloning, expression and function in tumor progression and metastasis. Nat Med. 1999; 5:793–802. [PubMed: 10395325]
13. McKenzie E, Tyson K, Stamps A, Smith P, Turner P, Barry R, et al. Cloning and expression profiling of Hpa2, a novel mammalian heparanase family member. Biochem Biophys Res Commun. 2000; 276:1170–7. [PubMed: 11027606]
14. Levy-Adam F, Feld S, Cohen-Kaplan V, Shteingauz A, Gross M, Arvatz G, et al. Heparanase 2 interacts with heparan sulfate with high affinity and inhibits heparanase activity. J Biol Chem. 2010; 285:28010–9. [PubMed: 20576607]
15. Fong S, Debs RJ, Desprez PY. Id genes and proteins as promising targets in cancer therapy. Trends Mol Med. 2004; 10:387–92. [PubMed: 15310459]
16. Cohen-Kaplan V, Doweck I, Naroditsky I, Vlodavsky I, Ilan N. Heparanase augments epidermal growth factor receptor phosphorylation: correlation with head and neck tumor progression. Cancer Res. 2008; 68:10077–85. [PubMed: 19074873]

17. Cohen-Kaplan V, Jrbashyan J, Yanir Y, Naroditsky I, Ben-Izhak O, Ilan N, et al. Heparanase induces signal transducer and activator of transcription (STAT) protein phosphorylation: preclinical and clinical significance in head and neck cancer. J Biol Chem. 2012; 287:6668–78. [PubMed: 22194600]
18. Levy-Adam F, Abboud-Jarrous G, Guerrini M, Beccati D, Vlodavsky I, Ilan N. Identification and characterization of heparin/heparan sulfate binding domains of the endoglycosidase heparanase. J Biol Chem. 2005; 280:20457–66. [PubMed: 15760902]
19. Akiri G, Sabo E, Dafni H, Vadasz Z, Kartvelishvily Y, Gan N, et al. Lysyl oxidase-related protein-1 promotes tumor fibrosis and tumor progression in vivo. Cancer Res. 2003; 63:1657–66. [PubMed: 12670920]
20. Kutchuk L, Laitala A, Soueid-Bomgarten S, Shentzer P, Rosendahl AH, Eilot S, et al. Muscle composition is regulated by a Lox-TGFbeta feedback loop. Development. 2015; 142:983–93. [PubMed: 25715398]
21. Shteingauz A, Ilan N, Vlodavsky I. Processing of heparanase is mediated by syndecan-1 cytoplasmic domain and involves syntenin and alpha-actinin. Cell Mol Life sci. 2014; 71:4457–70. [PubMed: 24788042]
22. Adams RH, Alitalo K. Molecular regulation of angiogenesis and lymphangiogenesis. Nat Rev Mol Cell Biol. 2007; 8:464–78. [PubMed: 17522591]
23. Saharinen P, Tammela T, Karkkainen MJ, Alitalo K. Lymphatic vasculature: development, molecular regulation and role in tumor metastasis and inflammation. Trends Immunol. 2004; 25:387–95. [PubMed: 15207507]
24. Barry-Hamilton V, Spangler R, Marshall D, McCauley S, Rodriguez HM, Oyasu M, et al. Allosteric inhibition of lysyl oxidase-like-2 impedes the development of a pathologic microenvironment. Nat Med. 2010; 16:1009–17. [PubMed: 20818376]
25. Rodriguez C, Rodriguez-Sinovas A, Martinez-Gonzalez J. Lysyl oxidase as a potential therapeutic target. Drug News Perspect. 2008; 21:218–24. [PubMed: 18560621]
26. Doweck I, Kaplan-Cohen V, Naroditsky I, Sabo E, Ilan N, Vlodavsky I. Heparanase localization and expression by head and neck cancer: correlation with tumor progression and patient survival. Neoplasia. 2006; 8:1055–61. [PubMed: 17217623]
27. Barker HE, Cox TR, Erler JT. The rationale for targeting the LOX family in cancer. Nat Rev Cancer. 2012; 12:540–52. [PubMed: 22810810]
28. Lyden D, Young AZ, Zagzag D, Yan W, Gerald W, O'Reilly R, et al. Id1 and Id3 are required for neurogenesis, angiogenesis and vascularization of tumour xenografts. Nature. 1999; 401:670–7. [PubMed: 10537105]
29. Barash U, Zohar Y, Wildbaum G, Beider K, Nagler A, Karin N, et al. Heparanase enhances myeloma progression via CXCL10 downregulation. Leukemia. 2014; 28:2178–87. [PubMed: 24699306]
30. Boyango I, Barash U, Naroditsky I, Li JP, Hammond E, Ilan N, et al. Heparanase cooperates with Ras to drive breast and skin tumorigenesis. Cancer Res. 2014; 74:4504–14. [PubMed: 24970482]
31. Shteingauz A, Boyango I, Naroditsky I, Hammond E, Gruber M, Doweck I, et al. Heparanase enhances tumor growth and chemoresistance by promoting autophagy. Cancer Res. 2015; 75:3946–57. [PubMed: 26249176]
32. Zhang X, Xu S, Tan Q, Liu L. High expression of heparanase-2 is an independent prognostic parameter for favorable survival in gastric cancer patients. Cancer Epidemiol. 2013; 37:1010–3. [PubMed: 24139593]
33. Yu M, Liu L, Liang C, Li P, Ma X, Zhang Q, et al. Intratumoral vessel density as prognostic factors in head and neck squamous cell carcinoma: a meta-analysis of literature. Head Neck. 2014; 36:596–602. [PubMed: 23780885]
34. Alitalo K, Carmeliet P. Molecular mechanisms of lymphangiogenesis in health and disease. Cancer Cell. 2002; 1:219–27. [PubMed: 12086857]
35. Benezra R, Rafii S, Lyden D. The Id proteins and angiogenesis. Oncogene. 2001; 20:8334–41. [PubMed: 11840326]

36. Dong Z, Wei F, Zhou C, Sumida T, Hamakawa H, Hu Y, et al. Silencing Id-1 inhibits lymphangiogenesis through down-regulation of VEGF-C in oral squamous cell carcinoma. Oral Oncol. 2011; 47:27–32. [PubMed: 21111670]
37. Sikder HA, Devlin MK, Dunlap S, Ryu B, Alani RM. Id proteins in cell growth and tumorigenesis. Cancer Cell. 2003; 3:525–30. [PubMed: 12842081]
38. Strait KA, Dabbas B, Hammond EH, Warnick CT, Iistrup SJ, Ford CD. Cell cycle blockade and differentiation of ovarian cancer cells by the histone deacetylase inhibitor trichostatin A are associated with changes in p21, Rb, and Id proteins. Mol Cancer Ther. 2002; 1:1181–90. [PubMed: 12479699]
39. Mokhtari S. Mechanisms of cyst formation in metastatic lymph nodes of head and neck squamous cell carcinoma. Diagn Pathol. 2012; 7:6. [PubMed: 22248307]
40. Zhao CM, Hayakawa Y, Kodama Y, Muthupalani S, Westphalen CB, Andersen GT, et al. Denervation suppresses gastric tumorigenesis. Sci Transl Med. 2014; 6:250ra115.
41. Woolf AS, Stuart HM, Roberts NA, McKenzie EA, Hilton EN, Newman WG. Urofacial syndrome: a genetic and congenital disease of aberrant urinary bladder innervation. Pediatr Nephrol. 2014; 29:513–8. [PubMed: 23832138]
42. Daly SB, Urquhart JE, Hilton E, McKenzie EA, Kammerer RA, Lewis M, et al. Mutations in HPSE2 cause urofacial syndrome. Am J Hum Genet. 2010; 86:963–9. [PubMed: 20560210]
43. Pang J, Zhang S, Yang P, Hawkins-Lee B, Zhong J, Zhang Y, et al. Loss-of-function mutations in HPSE2 cause the autosomal recessive urofacial syndrome. Am J Hum Genet. 2010; 86:957–62. [PubMed: 20560209]
44. Stuart HM, Roberts NA, Hilton EN, McKenzie EA, Daly SB, Hadfield KD, et al. Urinary tract effects of HPSE2 mutations. J Am Soc Nephrol. 2015; 26:797–804. [PubMed: 25145936]
45. Arvatz G, Shafat I, Levy-Adam F, Ilan N, Vlodavsky I. The heparanase system and tumor metastasis: is heparanase the seed and soil? Cancer Metastasis Rev. 2011; 30:253–68. [PubMed: 21308479]
46. Guo C, Kaneko S, Sun Y, Huang Y, Vlodavsky I, Li X, et al. A mouse model of urofacial syndrome with dysfunctional urination. Hum Mol Genet. 2015; 24:1991–9. [PubMed: 25510506]
47. Bais MV, Ozdener GB, Sonenshein GE, Trackman PC. Effects of tumor-suppressor lysyl oxidase propeptide on prostate cancer xenograft growth and its direct interactions with DNA repair pathways. Oncogene. 2015; 34:1928–37. [PubMed: 24882580]
48. Zhan P, Shen XK, Qian Q, Zhu JP, Zhang Y, Xie HY, et al. Down-regulation of lysyl oxidase-like 2 (LOXL2) is associated with disease progression in lung adenocarcinomas. Med Oncol. 2012; 29:648–55. [PubMed: 21519871]
49. Li TY, Xu LY, Wu ZY, Liao LD, Shen JH, Xu XE, et al. Reduced nuclear and ectopic cytoplasmic expression of lysyl oxidase-like 2 is associated with lymph node metastasis and poor prognosis in esophageal squamous cell carcinoma. Hum Pathol. 2012; 43:1068–76. [PubMed: 22204712]
50. Iturbide A, Garcia de Herreros A, Peiro S. A new role for LOX and LOXL2 proteins in transcription regulation. FEBS J. 2015; 282:1768–73. [PubMed: 25103872]
51. Scherz-Shouval R, Santagata S, Mendillo ML, Sholl LM, Ben-Aharon I, Beck AH, et al. The reprogramming of tumor stroma by HSF1 is a potent enabler of malignancy. Cell. 2014; 158:564–78. [PubMed: 25083868]
52. Lugassy J, Zaffryar-Eilot S, Soueid S, Mordoviz A, Smith V, Kessler O, et al. The enzymatic activity of lysyl oxidas-like-2 (LOXL2) is not required for LOXL2-induced inhibition of keratinocyte differentiation. J Biol Chem. 2012; 287:3541–9. [PubMed: 22157764]
53. Roberts NA, Woolf AS, Stuart HM, Thuret R, McKenzie EA, Newman WG, et al. Heparanase 2, mutated in urofacial syndrome, mediates peripheral neural development in Xenopus. Hum Mol Genet. 2014; 23:4302–14. [PubMed: 24691552]
54. Cox TR, Rumney RM, Schoof EM, Perryman L, Hoye AM, Agrawal A, et al. The hypoxic cancer secretome induces pre-metastatic bone lesions through lysyl oxidase. Nature. 2015; 522:106–10. [PubMed: 26017313]
55. Levy-Adam F, Ilan N, Vlodavsky I. Tumorigenic and adhesive properties of heparanase. Semin Cancer Biol. 2010; 20:153–60. [PubMed: 20619346]

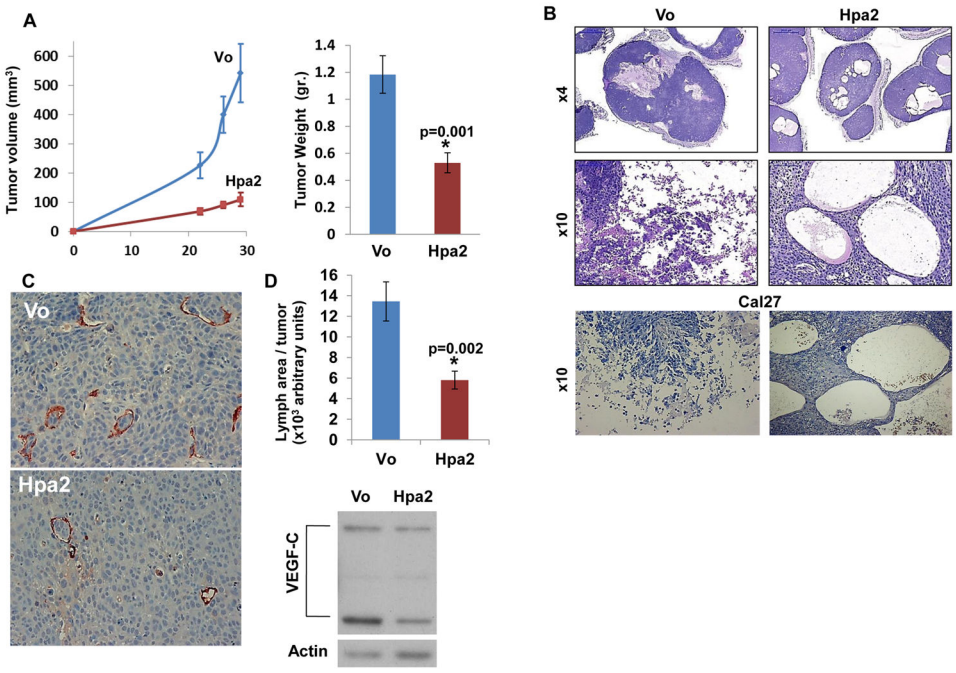

Figure 1.

Hpa2 over expression attenuates tumor growth. Control (Vo) and Hpa2 over expressing FaDu cells (5×10^6) were implanted subcutaneously in SCID mice and tumor volume was inspected (**A**, left). At termination, tumor xenografts were collected, weighed (**A**, right) and formalin-fixed. Paraffin-embedded 5 micron sections were subjected to histological examination. Shown are representative images of hematoxylin & eosin (H&E) staining at low (**B**, upper panel) and high (**B**, middle panel) magnifications. H&E staining of tumor xenografts produced by control (Vo) and Hpa2 over expressing Cal27 oral carcinoma cells is shown in B, lower panels. Note massive necrosis in control tumors vs. cysts structures in tumors over expressing Hpa2. Original magnifications: Upper panels ×4, middle and lower panels ×10. **C–D**. Lymph angiogenesis and VEGF-C expression. Five micron sections of tumor xenografts produced by control (Vo) and Hpa2 over expressing FaDu cells were stained with anti-LYVE-1 antibody, a marker for lymphatic endothelial cells (C); quantification of lymph vessel density is shown graphically in **D** (upper panel). Original magnification: ×40. Extracts of control and Hpa2 over expressing cells were subjected to immunoblotting applying anti-VEGF-C and anti-actin antibodies (D, lower panels).

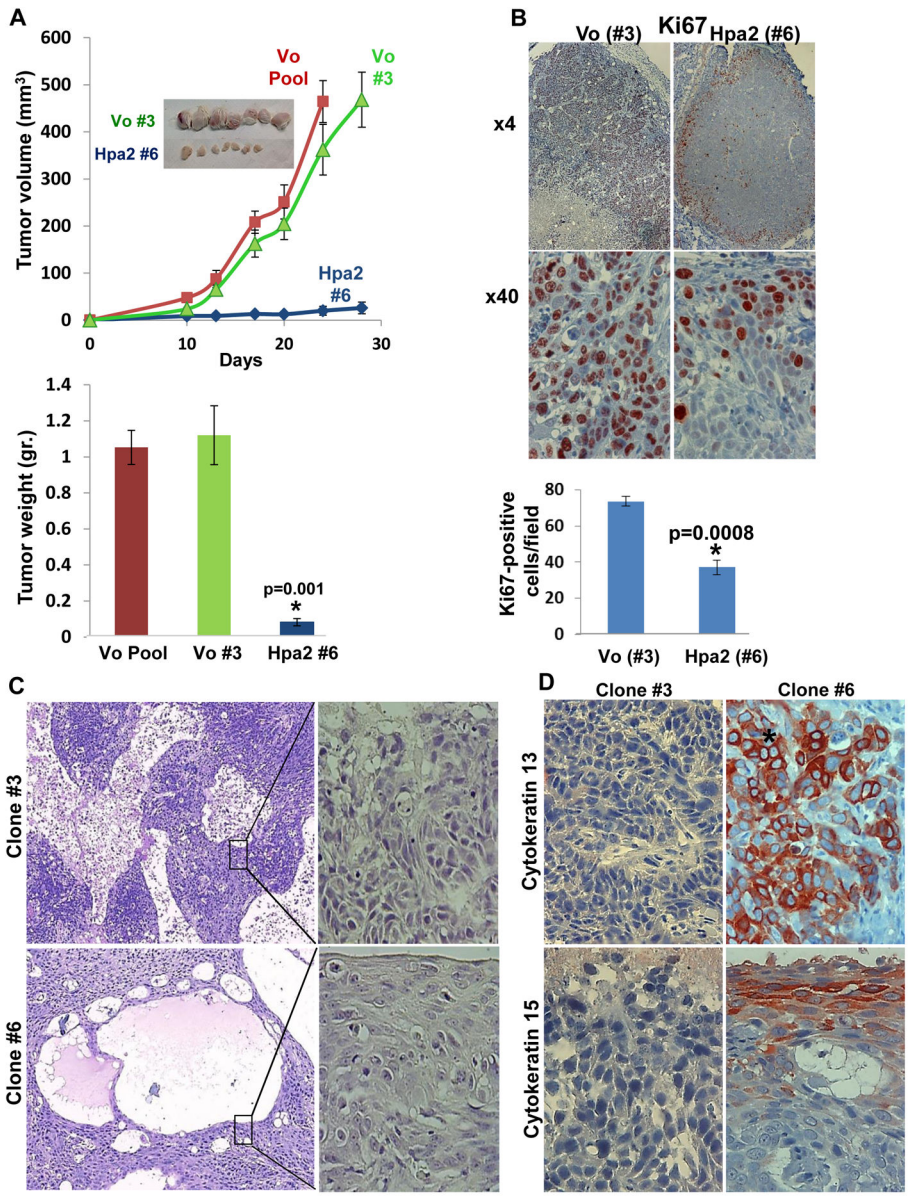

Figure 2.

Marked inhibition of tumor growth by Hpa2 over-expressing cell clones. Cell clones were isolated by limited dilution and clones that showed Hpa2 expression significantly higher than the cell pool were selected for subsequent experiments (#6, #60, #64). Three clones from control (Vo) cells were selected randomly (#3, #5, #8). **A**. Tumor growth. The indicated clone or pool cells were implanted subcutaneously in SCID mice and tumor growth was inspected over time (A, upper panel). At termination, tumors were collected, photographed (insets), weighed (A, lower panel) and fixed in formalin for histological evaluation. **B**. Cell proliferation. Five micron sections of control (Vo #3) and Hpa2 over expressing (#6) cell clones were subjected to immunostaining applying anti-Ki67 antibody. Shown are representative photomicrographs at low (×4; upper panels) and high (×40; lower panels) magnifications. Quantification of Ki67-positive cell is shown in the lower panel. **C–**

D. Cell differentiation. Five micron sections of tumor xenografts produced by control (#3) and Hpa2 over expressing (#6) cell clones were subjected to histological evaluation. Shown are representative photomicrographs of H&E staining at low (×4; C, left panels) and high (×40; C, right panels) magnifications. Sections were subjected to immunostaining applying anti-cytokeratin 13 (D, upper panels) and cytokeratin 15 (D, lower panels) antibodies. Note, increased differentiation of tumor cells over expressing Hpa2. Original magnifications: ×40.

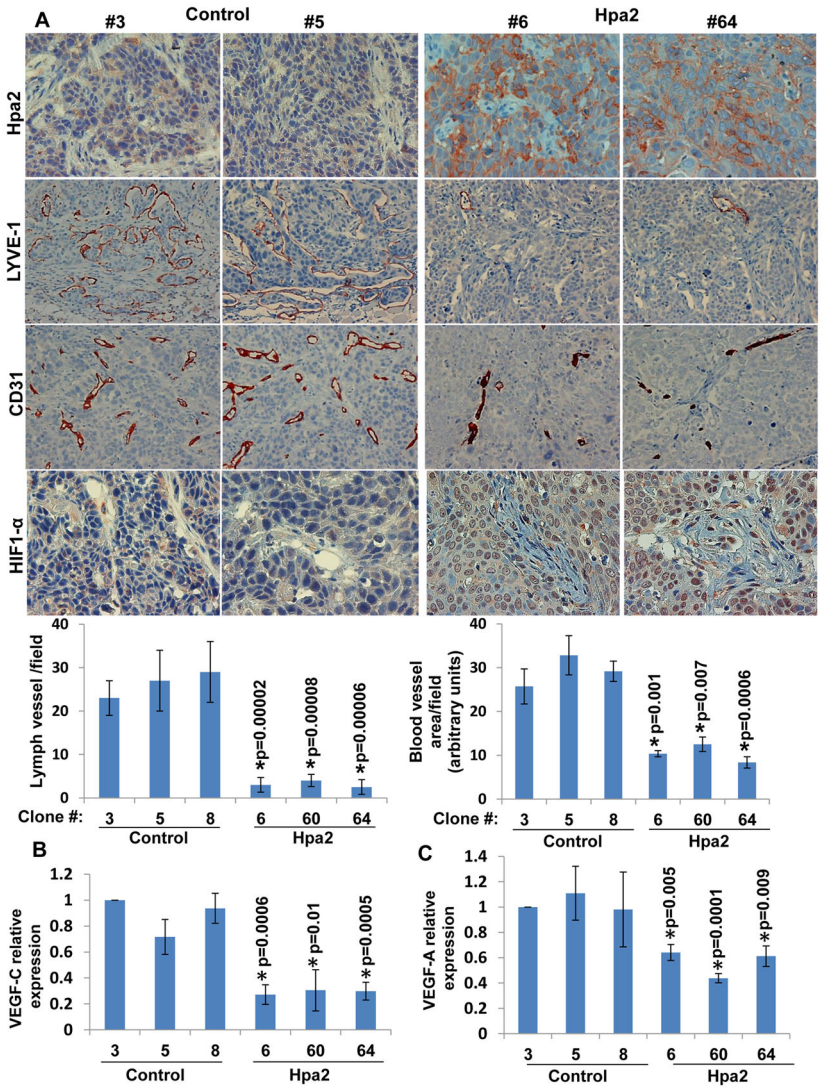

Figure 3.

Hpa2 over expression is associated with decreased tumor vascularity. **A**. Immunostaining. Sections of tumor xenografts produced by control (#3, #5) and Hpa2 over expressing (#6, #64) cell clones were subjected to immunostaining applying anti-Hpa2 (upper panels), anti-LYVE-1 (second panels), anti-CD31 (third panels), and anti-HIF-1α (fourth panels) antibodies. Note, reduced tumor vascularity and increased tumor hypoxia following Hpa2 over expression. Original magnifications: upper, third and fourth panels ×40, second panels ×20. Quantification of lymph (LYVE-1-positive) and blood (CD31-positive) vessels is shown graphically in the lower panels. **B–C**. Real time PCR. Total RNA was extracted from the indicated cell clones and corresponding cDNAs were subjected to quantitative real-time PCR analyses. Expression of VEGF-C (B) and VEGF-A (C) are presented graphically in relation to the levels in control clone #3, set arbitrarily to a value of 1.

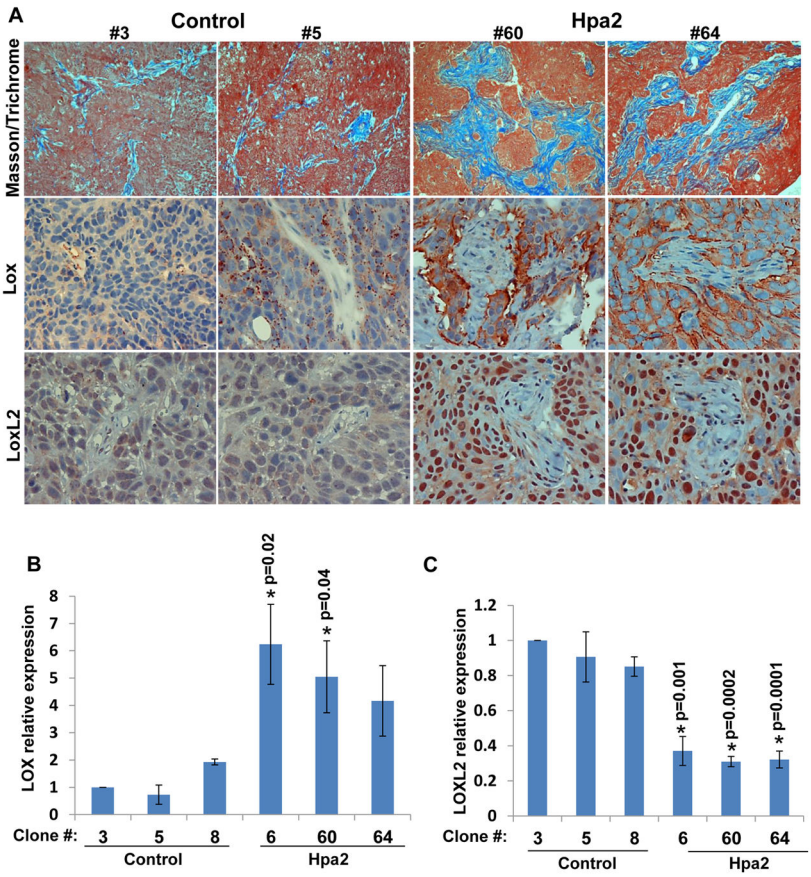

Figure 4.

Hpa2 induces LOX expression and LOXL2 nuclear localization. **A**. Masson's/Trichrome and immunostaining. Five micron sections from tumor xenografts produced by the indicated control (#3, #5) and Hpa2 over expressing (#60, #64) cell clones were stained with Masson's/Trichrome reagents (upper panels). Blue staining denotes collagen type I deposition. Corresponding tumor sections were subjected to immunostaining applying anti-LOX (second panels) and anti-LOXL2 (third panels) antibodies. Note increased collagen deposition by cells over expressing Hpa2, associating with increased LOX levels and nuclear localization of LOXL2. Original magnification: ×40. **B–C**. Real-time PCR. Total RNA was extracted from the indicated cell clones and corresponding cDNAs were subjected to quantitative real-time PCR analyses. Expression levels of LOX (B) and LOXL2 (C) are shown graphically in relation to the levels in control clone #3 set arbitrarily to a value of 1.

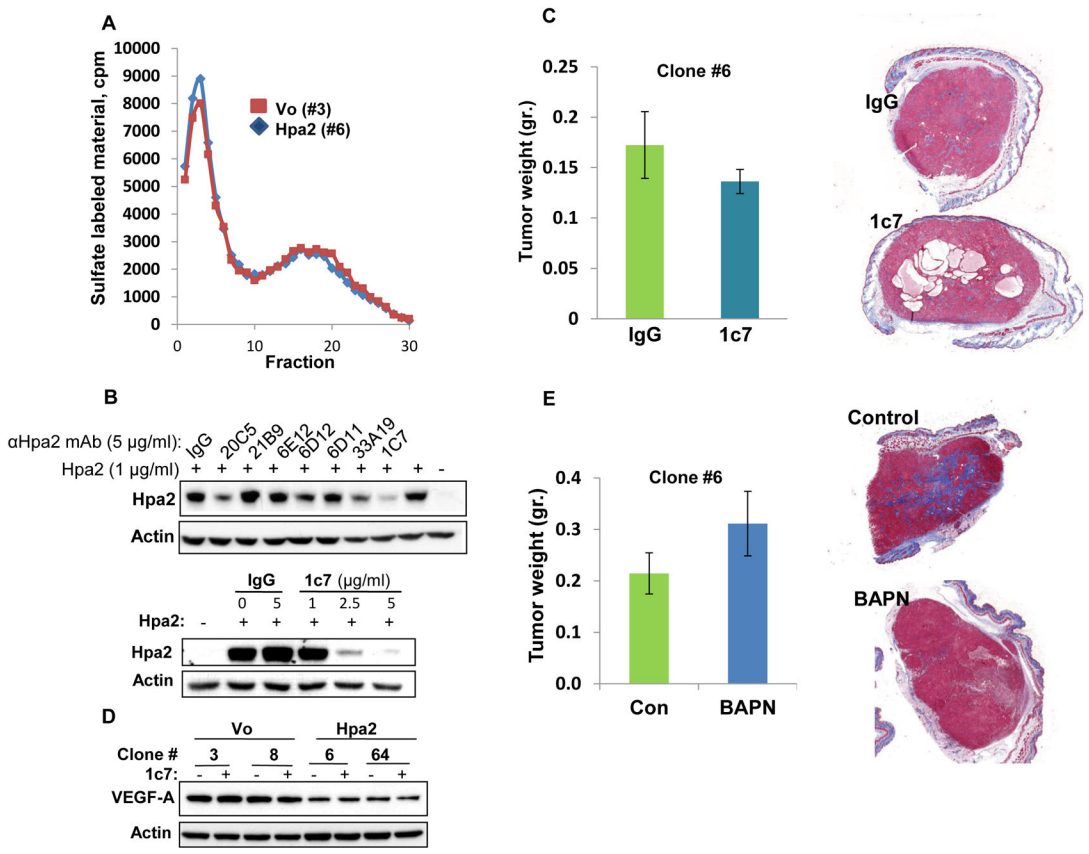

Figure 5.

Hpa2 mode of action. **A**. Heparanase activity. Control (#3) and Hpa2 over expressing (#6) cell clones were plated on dishes coated with sulfate-labelled ECM and grown for three days. Conditioned medium was then collected and evaluated for heparanase activity as described in 'Materials and Methods'. **B**. Characterization of monoclonal antibody (mAb) 1c7. Hpa2 (1 μg/ml) was added to 293 cells together with the indicated anti-Hpa2 mAb or control mouse IgG (5 μg/ml; 30 min, 37ºC) under serum-free conditions. Medium was then aspirated, cells were washed twice with PBS and lysate samples were subjected to immunoblotting applying anti-Hpa2 (upper panel) and anti-actin (second panel) antibodies. Decreased cellular binding of Hpa2 by mAb 1c7 is shown to be dose-dependent (third panel). **C**. Tumor xenografts. Hpa2 over expressing clone #6 cells were implanted (5×10^6) subcutaneously in SCID mice (n=7) and mice were administrated with mAb 1c7 (250 μg/mouse) three times a week. At termination, tumors were collected, weighed (left panels) and processed for histological examination. Shown are representative images of whole sections stained with Masson's/Trichrome reagents and scanned by 3DHISTECH Pannoramic MIDI System attached to HITACHI HV-F22 color camera (3dhistech kft, Budapest, Hungary). Note that mAb 1c7 does not affect tumor growth but appears to enhance cyst formation. **D**. VEGF-A expression. The indicated cell clones were incubated without (-) or with (+) mAb 1c7 (5 μg/ml, 18 h, 37ºC) and lysate samples were subjected to immunoblotting applying anti-VEGF-A (upper panel) and anti-actin (lower panel) antibodies. Note decreased VEGF-A levels in cells over expressing Hpa2, which is not affected by mAb 1c7. **E**. LOX inhibitor.

SCID mice (n=7) were inoculated subcutaneously with Hpa2 over expressing clone #6 cells (5×10^6) and mice were administrated with LOX inhibitor BAPN (0.75% in drinking water). At termination, tumors were collected, weighed (left panels) and processed for histological examination. Shown are representative images of whole sections stained with Masson's/ Trichrome reagents and scanned by 3DHISTECH Pannoramic MIDI System (right panels). Note that LOX inhibitor does not affect tumor growth but reduces tumor fibrosis (i.e., collagen content).

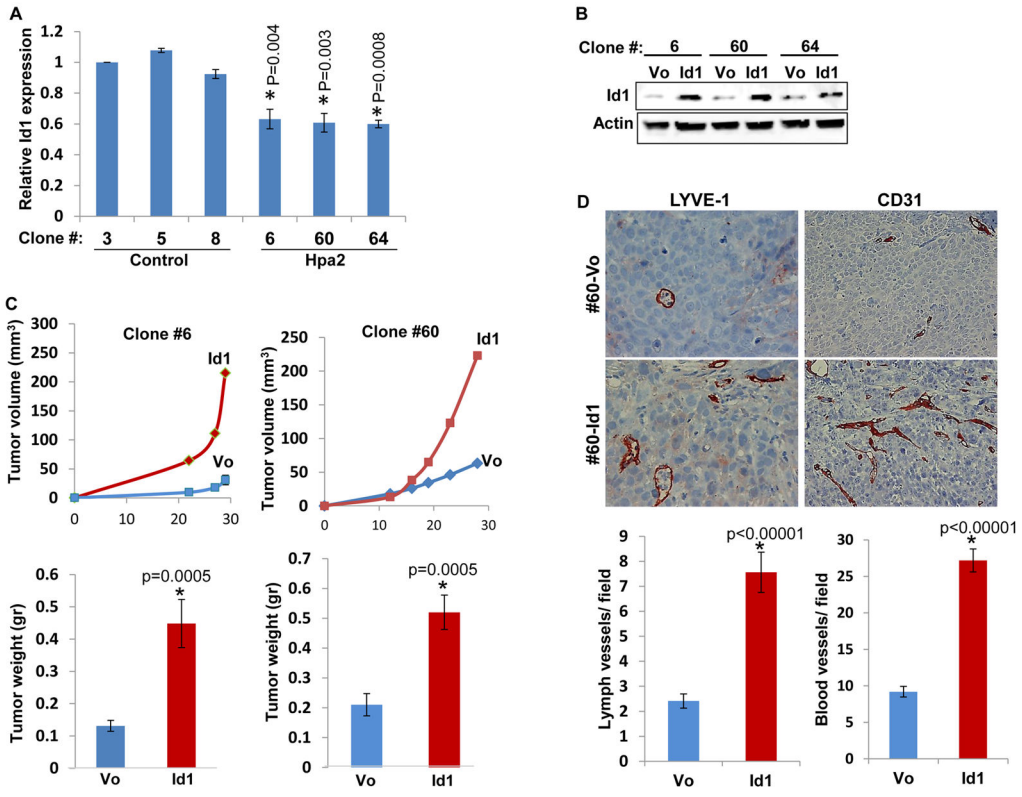

Figure 6.

Over expression of Id1 restores tumor growth and vascularity. **A**. Id1 expression. Real-time PCR analysis of Id1 expression in tumor xenografts produced by control (Vo) and Hpa2 over expressing cells. Expression of Id1 is presented graphically in relation to the levels in control clone #3, set arbitrarily to a value of 1. **B**. Id1 over expression. The indicated Hpa2 clone cells were stably transfected with Id1 gene construct (Addgene; Cambridge, MA) or control empty vector (Vo) and cell lysates were subjected to immunoblotting applying anti-Id1 (upper panel) and anti-actin (lower panel) antibodies. **C**. Tumor growth. Control (Vo) and Id1 over expressing cells were inoculated subcutaneously in SCID mice and tumor growth was inspected over time (upper panel). At termination, tumors were collected, weighed (lower panel) and processed for histological examination. **D**. Five micron sections of tumors produced by control (Vo) and Id1 over expressing clone #60 cells were subjected to immunostaining applying anti-LYVE-1 (left panels) and anti-CD31 (right panels) antibodies. Quantification of LYVE-1- and CD31-positive vessels is shown graphically in the lower panels. Original magnifications: left panels ×40, right panels ×20.